Observation of Dynamic Strain Hardening in Polymer Nanocomposites

Brent J. Carey,[†] Prabir K. Patra,[†,§] Lijie Ci,[†] Glaura G. Silva,[‡] and Pulickel M. Ajayan[†,*]

[†]Department of Mechanical Engineering & Materials Science, Rice University, Houston, Texas 77005, United States, and [‡]Department of Chemistry, Universidade Federal de Minas Gerais, Belo Horizonte, Minas Gerais 31270-901, Brazil. [§] Present address: Departments of Mechanical Engineering and Biomedical Engineering, University of Bridgeport, Bridgeport, Connecticut 06604, United States.

ABSTRACT Most materials respond either elastically or inelastically to applied stress, while repeated loading can result in mechanical fatigue. Conversely, bones and other biomechanical tissues have the ability to strengthen when subjected to recurring elastic stress. The cyclic compressive loading of vertically aligned carbon nanotube/poly(dimethylsiloxane) nanocomposites has revealed a self-stiffening response previously unseen in synthetic materials. This behavior results in a permanent increase in stiffness that continues until the dynamic stress is removed and resumes when it is reapplied. The effect is also specific to dynamic loads, similar to the localized self-strengthening that occurs in biological structures. These observations help to elucidate the complex interactions between matrix materials and nanostructures, and control over this mechanism could lead to the development of adaptable structural materials and active, load-bearing artificial connective tissues.

KEYWORDS: strain hardening · carbon nanotubes · nanocomposite · mechanical testing · cold crystallization

Most materials, when subjected to sufficient repeated mechanical stress, will undergo irreversible microstructural damage, which can lead to cracking, delamination, or other failure at stress levels below what they could previously bear. The additions of nanoscale ceramic particles, carbon nanotubes (CNTs), and even phase-separated poly(dimethylsiloxane) (PDMS) healing agents have recently been shown to result in polymer composites that have exhibited respectively crack pinning,[1] the suppression of microcrack propagation,[2] and self-healing,[3] thereby extending the fatigue life with little penalty. These referenced works focus on passively improving the resilience to dynamic loads above the fatigue limit (the minimum stress necessary to induce fatigue-related failure), while, alternatively, materials are sometimes reinforced or otherwise "strengthened" in order to improve their resiliency to repeated loading.

The act of strengthening through deformation is not new, although the mechanisms responsible are typically a preparatory measure and a result of plastically deforming a material to alter its microstructure and, in turn, its bulk properties. Strain hardening is a technique used predominantly in metallurgy where a greater density of dislocations (defects) are generated in the crystal structure through repeated plastic deformation; this mechanism results in a stronger material that resists further deformation. Alternatively, some biomechanical tissues *in vivo* can actively strengthen by adapting to the loads they are repeatedly subjected to. For example, regular elastic stress on bones will stimulate a localized increase in bone density, a response mechanism commonly referred to as Wolff's law, which reduces the risk of fracture in areas of frequent loading.

CNTs have recently been shown to be capable of biomimetic actuation,[4] and in a response strikingly similar to what occurs in bones, we report the observation of dynamic-stress-induced mechanical stiffening in CNT/PDMS nanocomposites. This behavior is a unique and not-yet-observed phenomenon similar in premise to strain hardening that, in contrast, occurs during repeated elastic deformation. The effect leads to a discernible increase in stiffness and storage modulus, with no obvious limit after one week (3.5 million cycles) of continuous stressing. The stiffness improvement appears to be stifled (but not eliminated) by further heat treatment, implying that while the level of polymer cross-linking may play a role, another mechanism is occurring. Analysis of the subambient cold crystallization behavior of this material shows not only that nanotubes seed crystallinity in this polymer (an observation in support of recent work with other semicrystalline polymers[5−8]) but that the dynamically stressed sample begins crystallizing almost immediately upon introduction to the temperature range where crystallization may occur, in contrast to the unstressed composite and particularly the neat polymer.

* Address correspondence to ajayan@rice.edu.

Received for review November 16, 2010 and accepted March 16, 2011.

Published online March 16, 2011
10.1021/nn103104g

Several groups have recently reported that the efficiency of interfacial load transfer is critically dependent on CNT/polymer chemistry and adhesion,[9−12] and the manner in which the matrix is interacting with interstitials such as CNTs plays a significant role in the level of improvement they provide. While a conclusive mechanism for the stiffness increase is not yet entirely clear, our observations suggest that, in the presence of CNTs, the morphology of a rubbery polymer evolves and becomes much more ordered during repeated elastic stressing, thereby improving mechanical interaction with the CNTs and, in turn, the bulk properties of the composite. Further resolution and exploitation of this effect may have significant implications in the development of smart, active materials that selectively stiffen where stressed, and the known biocompatibility of PDMS[13] makes this material a candidate for load-bearing artificial connective tissues that can adapt to the loads applied to them. Additionally, with the development of next-generation composites reinforced with CNTs[14] and other nanoscale constituents such as cellulose nanofibers[15] and ceramic nanoparticles,[16−18] the study of matrix/nanoparticle interfacial interaction is becoming especially significant in order to efficiently utilize the impressive properties of these nanomaterials. The further resolution of this mechanism may aid in the understanding of these interactions and contribute to the improved application of nanomaterials in polymer matrixes.

RESULTS AND DISCUSSION

Nanocomposite specimens were cut into rectangular blocks approximately 2.5 mm long × 1 mm wide × 1 mm thick, as illustrated in Figure SI-1. Vertically aligned forests of multiwalled CNTs (Figure SI-2) were grown by a well-documented vapor-phase chemical vapor deposition process[19] using ferrocene and xylene precursors. PDMS, a silicone elastomer, has an extreme affinity for the surface of CNTs[20] and was used to impregnate the as-grown CNT forests using the previously reported infiltration procedure,[21] a process that has also been used with other polymer matrixes such as epoxy,[22] poly(methyl methacrylate),[23] and poly(*N*-isopropylacrylamide).[24] We previously reported that these vertically aligned CNT/PDMS nanocomposites exhibit a clear anisotropy as well as impressive strength and damping as compared to the neat polymer.[21] Through the monotonic loading and low-cycle hysteresis behavior of this material, respectively, a 6-fold improvement in the modulus and up to a 21-fold increase in damping was observed.

With both aligned forests of CNTs[25] and polymer-infiltrated CNT composites[26] having been shown to display viscoelastic behavior, dynamic mechanical analysis (DMA) is an ideal tool, as it can be used to track the evolution of stiffness and viscoelastic properties such as the storage (E') and loss (E'') moduli and damping (tan δ) with great precision during dynamic stressing. Fundamental viscoelastic analysis of these composites is provided in Figure SI-3. By using DMA to subject the material to high-cycle loading, Figure 1c illustrates the stiffening phenomenon that occurs during dynamic compressive testing. Compared to the neat polymer (which shows no significant change), we observe up to a 7.5% improvement in the stiffness after one day of dynamic stressing. After one week (3.5 million cycles) of continuous dynamic stress and a 12% increase in stiffness, there is still no observable ceiling to this behavior, indicating that there is potential for even greater improvement. The anisotropy of these samples allows for two distinct responses based on the orientation of the sample during deformation, and by comparing these orientations for identical testing conditions in Figure 2a, we observe a 5.9% increase in stiffness when tested radially (transverse to CNT alignment) as compared to a 4.3% improvement axially (longitudinal to CNT alignment). The disparity in improvement suggests that, due to the mechanics of the deformation in the radial testing mode, nanotube/polymer interfacial pressure may play a role in explaining the behavior. Comparing the other viscoelastic properties in Figure SI-4, this stiffening is characterized by an increase in stiffness and storage modulus with a concurrent decrease in loss modulus and damping for the composites. Testing at various frequencies and strain amplitudes also exhibited the effect, and the phenomenon was also observed in randomly oriented CNT composites prepared two years ago,[21] signifying that this mechanism is not isolated to the specific experimental parameters used, the alignment of the CNTs, or fresh composites (Figure SI-5).

After exploring the limits by which to observe the phenomena for dynamic stress, the material was then tested with static loads to ascertain whether or not the stiffening would occur in the absence of cyclic loading. While stress relaxation testing (Figure 2b) revealed no increase in the relaxation modulus, the effects of such testing on the stiffness reported by the DMA during dynamic stress are not immediately apparent. To clearly delineate the contribution from both modes of deformation, a single sample was then subjected to alternating static and dynamic loads. In agreement with the stress relaxation testing, we see in Figure 2c that the static tests did not contribute to the stiffening, and furthermore, since the sample was allowed to recover in the ∼8 h between each of these tests, we note that there is a temporary relaxation that occurs at the offset of dynamic stressing. It is clear that the stiffness between each dynamic test begins at a lower value than the ending point of the previous one, but that it quickly resumes the path from the first test. Since each subsequent dynamic test shows a smaller drop, we posit that the temporary mechanism is recoverable

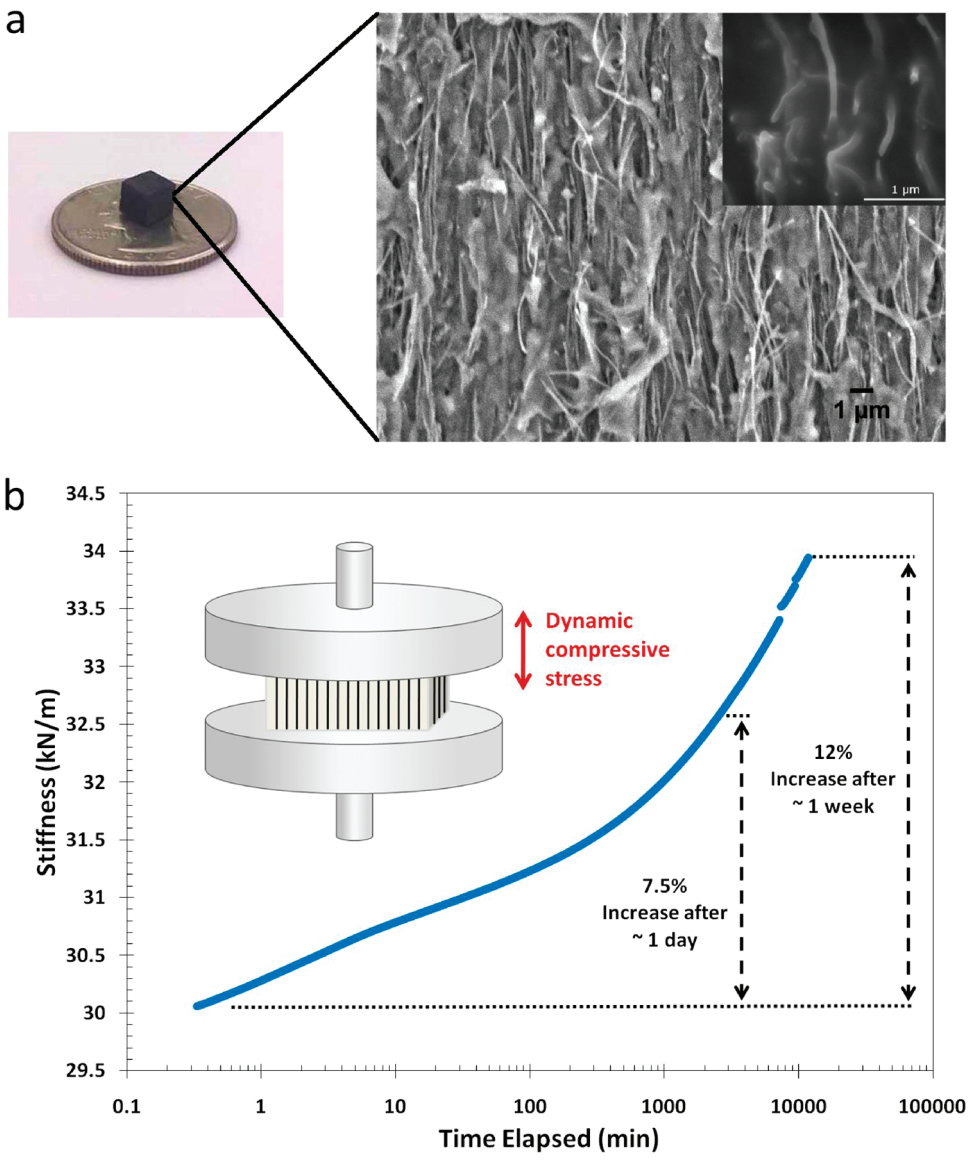

Figure 1. Evidence of dynamic stiffening in PDMS/CNT composites. (a) Continuously reinforced nanocomposites were prepared by infiltrating freestanding carbon nanotube (CNT) forests with poly(dimethylsiloxane) (PDMS) and curing *in situ*. (b) Discernable stiffening was observed for the composite during cyclic compressive stressing (inset), a phenomenon not observed for the neat polymer. This behavior was seen to continue even after one week and a total number of 3.5 million cycles, and the trend shows no obvious saturation or ceiling (the breaks in the test are a result of restarted tests due to furnace errors with the instrument). This stiffening was also observed in randomly aligned CNT composites prepared two years ago,[21] suggesting that it is not exclusive to vertically aligned CNTs or fresh composites. Harnessing this mechanism could have significant implications in the development of self-strengthening materials and improved nanocomposites.

and that there is a transition from temporary to permanent improvement during continuous stressing. This recoverability is also observed in samples that rested for only 10 min between dynamic tests, which implies that the partial relaxation occurs very quickly. Lastly, this test allowed us to confirm that the observed change in stiffness was truly a result of a change in the properties of the material and not a result of our samples dynamically creeping during testing. In Figure SI-6, we note that the sample displaced in the same manner during each static and dynamic test, eliminating any concern that a shifting zero point of oscillation was responsible for the perceived stiffness increase.

To begin to resolve the mechanism for this change in stiffness, it is necessary to further understand how changes in the polymer influence the effect. It was recently reported that the cross-linking mechanism near the CNT/polymer interface may be interrupted by the presence of the CNTs for epoxy[27] and silicone elastomer[28] matrixes, and the intent of the following experiment was to resolve the role that the degree of curing may play in explaining the stiffening phenomenon. Using the as-cured (1 h at 100 °C) composite as a control, an identical specimen was subjected to an additional 3 days of 100 °C heat treatment; by subjecting these samples to identical testing conditions, it

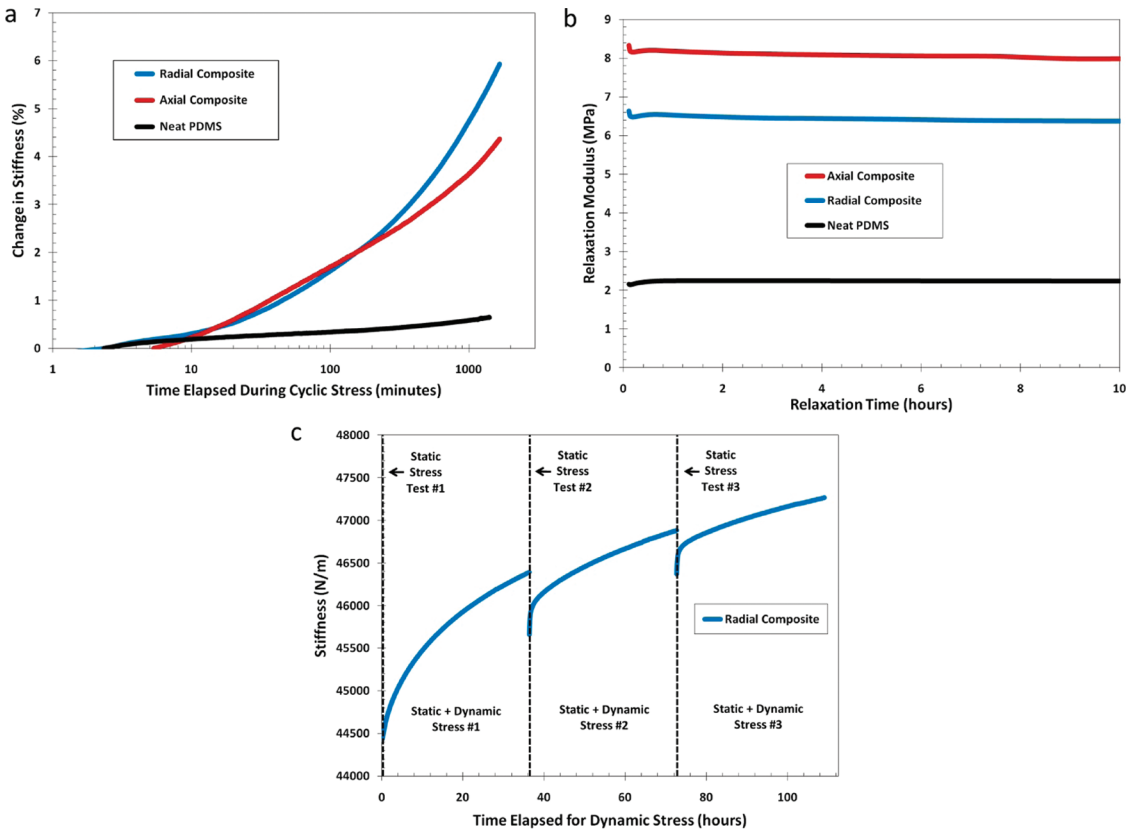

Figure 2. Comparing the testing orientation, and proof of permanent stiffening occurring only during dynamic stress. (a) There is no significant change in the neat polymer, and there is a heightened improvement when the composite is stressed transverse to the CNT alignment direction; this observation suggests that interfacial pressure promotes the stiffening. (b) Stress relaxation testing for a displacement similar to what is endured during the dynamic tests showed no improvement, indicating that dynamic stress is necessary to initiate the change. (c) To observe the effects that static stress and recovery have on the stiffening, a single sample was subjected to 3 bouts of 1 MPa static stress each followed by a dynamic test using the same static load with the addition of a 5% strain amplitude. There is an obvious retention of stiffness between tests, and while there is some temporary relaxation between dynamic tests, it quickly resumes the previous trend. The amplitude of that relaxation appears to diminish over extended testing, suggesting that there is a transition from temporary to permanent improvement. There is also clearly no contribution due to the static tests, confirming that this is a cumulative response that is exclusive to dynamic stressing.

allows us to differentiate between the stiffening behavior and any changes occurring exclusively due to further chemical changes in the polymer (cross-linking). A set of these samples were dynamically tested at 45 °C (Figure 3a), and we observe that while the percent improvement is greater for the as-cured sample, we still do very much observe the stiffening in the sample that can be considered close to fully cured. When dynamically stressed in a 100 °C environment (Figure 3b), it is obvious that the heat-treated sample began its dynamic test with a greater storage modulus due to the extended curing it underwent prior to testing, but that its ultimate improvement is less than the sample that was dynamically stressed during its first exposure to extended heating. This observation is particularly interesting since the heat-treated sample was ultimately subjected to the 100 °C environment for twice as long as the as-cured sample, further strengthening the argument that this effect is not simply a result of further cross-linking of the polymer. From these experiments and observations, we draw the following conclusions: (1) the composites are not fully cured after the recommended curing regimen (in agreement with the aforementioned work[27,28]), and (2) while the cross-link density may be correlated to the heightened improvement observed in the as-cured samples, something other than increased cross-linking must be responsible for the stiffening.

In addition to affecting the curing kinetics, it is known that interstitials (and particularly those with nanoscale dimensions) can have profound effects on the morphology of polymers. To probe this, the thermomechanical behavior of polymers can be used to resolve the kinetics of their second-order phase transitions and other thermodynamic events to expose subtle structural nuances that may be difficult to detect through microscopy or spectroscopy. The heights of the two major second-order phase transitions in this polymer, the α (glass) and α* (crystal−crystal slip) transitions, represent respectively the relative quantities of the amorphous and crystalline regions that exist in the sample. In Figure 4a we see that at room

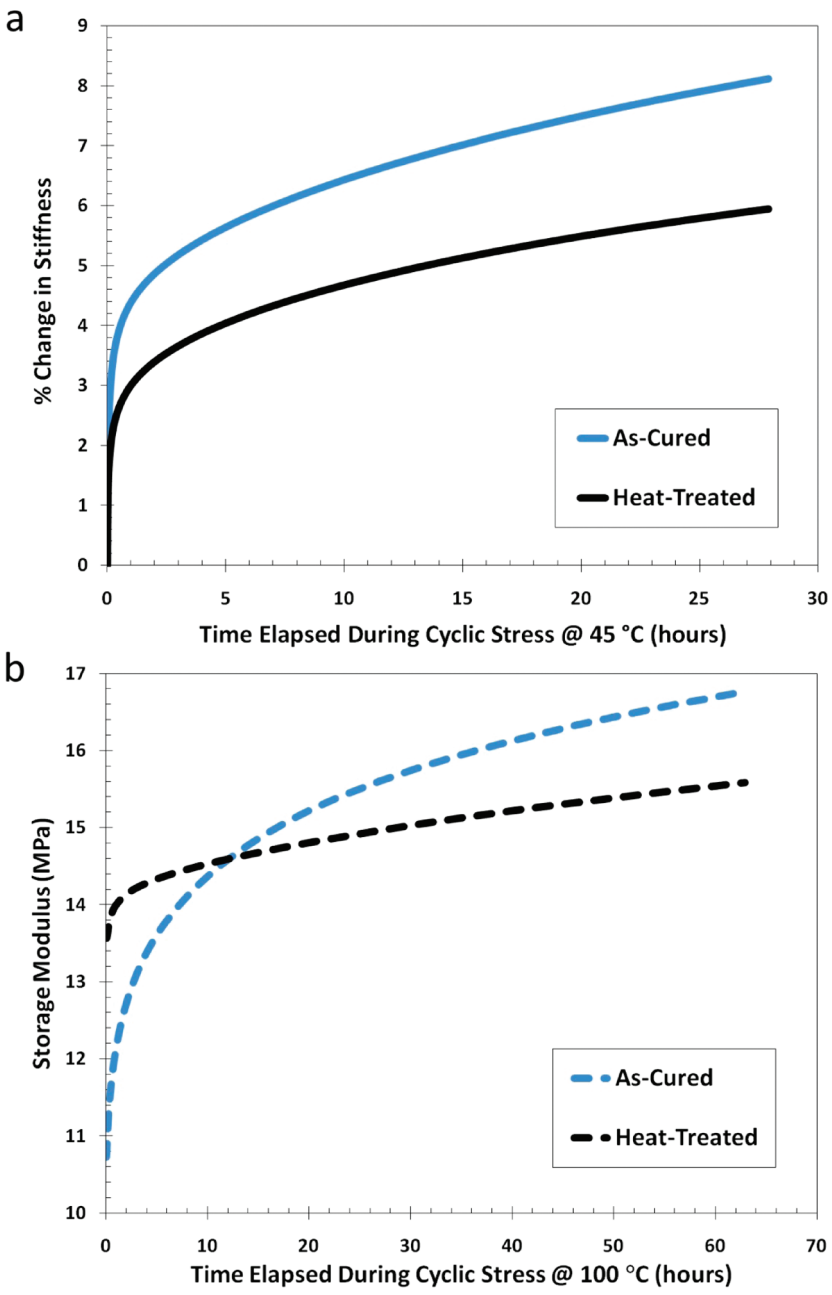

Figure 3. Effect of extended curing on the stiffening. The comparison of samples that were tested as-cured to those given 3 days of heat treatment at 100 °C prior to dynamic stressing displays the significant effect changes in the polymer chemistry (cross-linking) may be having on the stiffening. (a) When the samples are tested at 45 °C, the as-cured sample shows a greater improvement during dynamic stressing, yet the effect still occurs in the heat-treated sample. (b) While the heat-treated sample begins at a greater storage when tested at 100 °C, it does not have the same potential since its chains are more confined. These results indicate that while chemical changes in the polymer may play some role, another mechanism is responsible.

temperature PDMS is largely amorphous, which, coupled with the limberness of the polymer chains and the chain-end cross-linking in this particular PDMS, accounts for its ability to deform elastically to very large strains. PDMS is also known to cold crystallize[29] in the temperature range of approximately −100 to −70 °C, and by isothermally holding the samples in this temperature range during testing, we can probe the rate of crystallization and, afterward, any evolution of the transitions as a result.

Comparing the transitions in the neat polymer samples and the composites that have been subjected to various stresses, there are no distinct differences between the position and shape of these two peaks between all of the samples both before (Figure 4a) and after (Figure 4b) cold crystallization; this suggests that the CNTs are not coalescing[30] and that they are not altering the steady-state degree of crystallinity in the polymer. However, there is a very significant difference in the way each of these samples cold crystallizes,

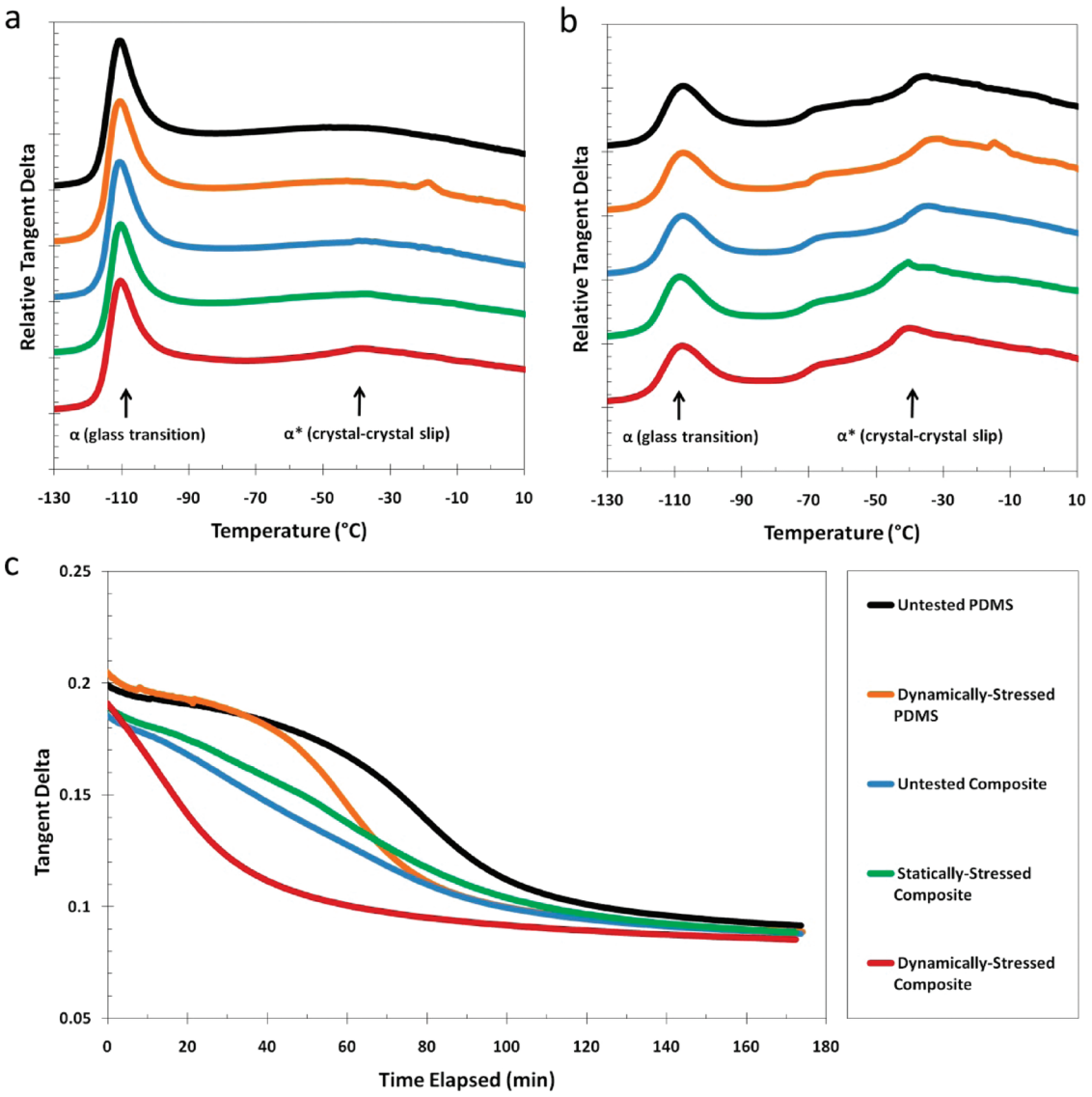

Figure 4. Observance of rapid cold crystallization after dynamic stress. Thermal transitions in the polymer, such as the α (glass) transition, which indicates amorphous structure, and the α* transition, which represents crystal−crystal slip, are identical (a) before and (b) after cold crystallization takes place, suggesting that the CNTs are not coalescing[30] and that the amount of steady-state crystallinity in the sample has not changed. (c) The rate at which crystallization occurs, however, varies greatly between each sample. The unstressed and statically stressed composites begin crystallizing much earlier than both the unstressed and dynamically stressed neat polymer samples, while the dynamically stressed composite begins crystallizing immediately upon entering the temperature regime where crystallization can occur. This result indicates increased polymer chain alignment/organization that is induced by the dynamic stressing of the composite; such organization has been attributed to improved interfacial load transfer in CNT nanocomposites[34] and, as such, is a likely explanation for the improvement in stiffness that we observe.

revealing information regarding the morphology of the polymer in these samples. The evolution of the damping in the samples during cold crystallization (Figure 4c) allows us to resolve the rate at which the crystallites are forming, and we see that both the unstressed and dynamically stressed neat PDMS samples take ∼40 min to begin crystallizing, a result that is explained by the fact that it takes time for the PDMS chains to kinetically arrange in order to form the crystallites. In contrast, the unstressed and statically stressed composites begin crystallizing much earlier, indicating that the presence of the CNTs seeds the polymer crystals.

CNTs have been shown to considerably affect the polymorphism of the polymer matrix and have been reported to affect the crystallization temperature, broaden the crystallite size distribution, and even promote the formation of other thermodynamically stable crystal phases.[31] The specific observation of nanostructure-induced polymer crystallinity has been reported for several semicrystalline polymer matrixes,[5−8] is supported by a recent molecular dynamics study reporting polymer crystallization in the presence of nanoscale particles,[32] and was observed specifically in PDMS by Dollase *et al.*, where ∼250 nm agglomerates

of 10−20 nm-in-diameter fumed silica particles were observed to locally enhance its cold crystallization.[33] While the CNTs are clearly having an effect on the morphology of the amorphous polymer, the more interesting result from Figure 4c is that the dynamically stressed sample begins crystallizing immediately upon being introduced to the temperature range where crystallization can occur, indicating that the polymer chains are even more organized in this sample, allowing them to rapidly form crystallites. The pre- and postcrystallization thermal scans are identical for differential scanning calorimetry (DSC) as seen in Figure SI-7, and the above observation that there is a change in the polymer after dynamic stressing is reinforced by thermogravimetric analysis (TGA) in Figure SI-8.

Recently, Coleman *et al.* proposed that a thicker crystallized shell around CNTs could improve bulk composite strength for semicrystalline polymers,[6] a phenomenon that they suggested was a potentially beneficial side effect of the presence of CNTs in polymers. In 2004, modeling by Wei, Srivastava, and Cho gave evidence for the formation of distinct polymer adsorption layers around CNTs in polyethylene, and their work went on to suggest that well-oriented layers of the polymer at the interface would contribute to enhanced van der Waals interaction with the CNT and, subsequently, better load transfer from the matrix to the nanotube reinforcement.[34]

From the observations above, we conjecture that additional chain alignment along the PDMS/CNT interface is responsible for the observed stiffening. The organization of the polymer chains in the interfacial or interphasic region would lead to greater physical interaction with the CNTs and a higher bulk stiffness, and such orientation would account for the dynamically stressed sample's readiness to crystallize as compared to all of the other samples. This is a feasible mechanism even for a fully cured composite since this particular PDMS (Sylgard 184) cross-links only at its ends, leaving a long uninterrupted chain that can freely translate. Additionally, the importance of chain mobility in explaining this mechanism is also perhaps supported by the fact that this behavior has not been observed previously in the fatigue testing of glassy CNT nanocomposites;[2] in the glassy state, polymer chains are "frozen" in place and exhibit much less local mobility.

This intriguing behavior not only gives new insight into the CNT/polymer interfacial region but could be utilized as a technique, similar in practice to strain hardening, to noninvasively improve the mechanical properties of nanocomposites. Perhaps most significantly, we note that the lack of an obvious upper limit to the effect and the enhanced improvement in the as-cured samples as noted in Figure 3 highlight the potential for even greater improvement if this mechanism can be harnessed and deliberately applied. Our observations should have implications in the development of new adaptable materials that can stiffen where they are repeatedly stressed, and further study of this phenomenon could lead to the improved engineering of load transfer in polymer nanocomposites and the understanding of new modes of polymer/nanoparticle interactions in nanoscale hybrid materials.

METHODS

Carbon Nanotube Synthesis. Ferrocene/xylene chemical vapor deposition[19] was used to grow the vertically aligned CNT forests for these composites (Figure SI-2). These forests are loosely packed (∼5% volume), have large (∼50−100 nm) diameters due to their many-walled structure, and are several millimeters in length, making it easy to prepare and handle macroscopic specimens.

Composite Preparation. The CNT forests were vacuum-infiltrated with the PDMS precure in a method identical to the one used in the publication introducing this material.[21] Sylgard 184 (Dow Corning), a commercially available, end-linked PDMS, was prepared at the recommended 10:1 weight ratio of monomer:curing agent. After ensuring homogeneous dispersion by manually stirring for at least 5 min, a free-standing forest of vertically aligned carbon nanotubes (approximately 5% volume CNTs) is placed on top of the viscous mixture and allowed to become submerged by scooping excess prepolymer on top of the sinking forest. To expedite the infiltration, the specimen is then held in a vacuum of 1 Torr for at least 3 h, where proof of infiltration and is confirmed by the expulsion of bubbles from the forest due to the interstitial air being forced out. When all bubbling has ceased (approximately 3 h), the seamlessly impregnated composite is subjected to 100 °C heat treatment for 1 h, as per the instructions for full curing. The resultant composite can then be separated from the surrounding neat polymer by manually cutting with a razor blade.

Dynamic Mechanical Testing. The specimens were hand-cut with a razor blade, and only samples whose thickness and cross-sectional area were within 10% of the ideal were used. Dynamic compressive testing as illustrated in Figure 1b was conducted on a TA Instruments Q800 DMA at a 5% strain amplitude and at a frequency of 5 Hz (unless otherwise noted), which allowed for significant cyclic compressive loading without any risk of resonant or inertial effects (as per Figure SI-3). All tests were conducted isothermally at 45 °C in order to maintain a stable temperature profile without the use of liquid N_2, though the described behavior was observed for ambient temperature testing as well.

Stress Relaxation Testing. Using the Q800 and samples identical to those used for dynamic testing, stress relaxation testing was conducted at 10% strain at 45 °C.

Alternating Static and Dynamic Testing. Using the Q800, the sample was first subjected to a 1 MPa constant load for approximately one day, which is fundamentally a creep test. Without removing the sample or otherwise disturbing it (to ensure consistency between tests), the same sample was then subjected to an identical static load with an added 5% strain amplitude. There was no load applied to the sample during the ∼8 h in between each test, so the effects of recovery are also observed.

Cold Crystallization Testing. On the Q800, very small specimens (0.5 mm long × 0.5 mm wide × 1.25 mm thick) were tested radially at 2 Hz with a very small amplitude (0.3% strain) in order to remain below the stiffness limit of the instrument when passing through the T_g. These measures were necessary due to

the fact that compression was the only viable method as a result of the length limitations of the aligned CNTs. Samples were quickly cooled to −145 °C, then scanned at 5 °C/min up to 50 °C for the precrystallization thermal scan, then cooled and held at −90 °C for three hours to observe the cold crystallization, and finally cooled again to −145 °C before ramping at 5 °C/min up to 50 °C again for the postcrystallization thermal scan. The data presented in Figure 4 show the glass transition at ∼−109 °C due to the thermal lag during heating. The average T_g for these samples is ∼−117 °C.

Acknowledgment. The authors would like to acknowledge the NASA Graduate Student Researchers Program (GSRP) for support, as well as funding provided by Rice University.

Supporting Information Available: Basic viscoelastic analysis of the composite material, observation of stiffening under various strains and frequencies, and supplemental thermal analysis is available free of charge *via* the Internet at http://pubs.acs.org.

REFERENCES AND NOTES

1. Wetzel, B.; Rosso, P.; Haupert, F.; Friedrich, K. Epoxy Nanocomposites−Fracture and Toughening Mechanisms. *Eng. Fract. Mech.* **2006,** *73*, 2375–2398.
2. Zhang, W.; Picu, R. C.; Koratkar, N. Suppression of Fatigue Crack Growth in Carbon Nanotube Composites. *Appl. Phys. Lett.* **2007,** *91*, 193109.
3. Cho, S. H.; Andersson, H.; White, S.; Sottos, N.; Braun, P. Polydimethylsiloxane-Based Self-Healing Materials. *Adv. Mater.* **2006,** *18*, 997–1000.
4. Aliev, A. E.; Oh, J.; Kozlov, M. E.; Kuznetsov, A. A.; Fang, S.; Fonseca, A. F.; Ovalle, R.; Lima, M. D.; Haque, M. H.; Gartstein, Y. N.; *et al*. Giant-Stroke, Superelastic Carbon Nanotube Aerogel Muscles. *Science* **2009,** *323*, 1575–1578.
5. Assouline, E.; Lustiger, A.; Barber, A. H.; Cooper, C. A.; Klein, E.; Wachtel, E.; Wagner, H. D. Nucleation Ability of Multiwall Carbon Nanotubes in Polypropylene Composites. *J. Polym. Sci., Polym. Phys.* **2003,** *41*, 520–527.
6. Coleman, J. N.; Cadek, M.; Ryan, K. P.; Fonseca, A.; Nagy, J. B.; Blau, W. J.; Ferreira, M. S. Reinforcement of Polymers with Carbon Nanotubes. The Role of an Ordered Polymer Interfacial Region. Experiment and Modeling. *Polymer* **2006,** *47*, 8556–8561.
7. Cadek, M.; Coleman, J. N.; Barron, V.; Hedicke, K.; Blau, W. J. Morphological and Mechanical Properties of Carbon-Nanotube-Reinforced Semicrystalline and Amorphous Polymer Composites. *Appl. Phys. Lett.* **2002,** *81*, 5123–5125.
8. Zhang, S.; Minus, M. L.; Zhu, L.; Wong, C.; Kumar, S. Polymer Transcrystallinity Induced by Carbon Nanotubes. *Polymer* **2008,** *49*, 1356–1364.
9. Ramanathan, T.; Abdala, A. A.; Stankovich, S.; Dikin, D. A.; Herrera-Alonso, M.; Piner, R. D.; Adamson, D. H.; Schniepp, H. C.; Chen, X.; Ruoff, R. S.; *et al*. Functionalized Graphene Sheets for Polymer Nanocomposites. *Nat. Nanotechnol.* **2008,** *3*, 327–331.
10. Hou, Y.; Tang, J.; Zhang, H.; Qian, C.; Feng, Y.; Liu, J. Functionalized Few-Walled Carbon Nanotubes for Mechanical Reinforcement of Polymeric Composites. *ACS Nano* **2009,** *3*, 1057–1062.
11. Ajayan, P. M.; Schadler, L. S.; Braun, P. V. *Nanocomposite Science and Technology*; Wiley-VCH: New York, 2003.
12. Barber, A. H.; Cohen, S. R.; Wagner, H. D. Measurement of Carbon Nanotube−Polymer Interfacial Strength. *Appl. Phys. Lett.* **2003,** *82*, 4140–4142.
13. McDonald, J. C.; Whitesides, G. M. Poly(dimethylsiloxane) as a Material for Fabricating Microfluidic Devices. *Acc. Chem. Res.* **2002,** *35*, 491–499.
14. Moniruzzaman, M.; Winey, K. I. Polymer Nanocomposites Containing Carbon Nanotubes. *Macromolecules* **2006,** *39*, 5194–5205.
15. Capadona, J. R.; Shanmuganathan, K.; Tyler, D. J.; Rowan, S. J.; Weder, C. Stimuli-Responsive Polymer Nanocomposites Inspired by the Sea Cucumber Dermis. *Science* **2008,** *319*, 1370–1374.
16. Podsiadlo, P.; Kaushik, A. K.; Arruda, E. M.; Waas, A. M.; Shim, B. S.; Xu, J.; Nandivada, H.; Pumplin, B. G.; Lahann, J.; Ramamoorthy, A.; *et al*. Ultrastrong and Stiff Layered Polymer Nanocomposites. *Science* **2007,** *318*, 80–83.
17. Koerner, H.; Misra, D.; Tan, A.; Drummy, L.; Mirau, P.; Vaia, R. Montmorillonite-Thermoset Nanocomposites via Cryo-Compounding. *Polymer* **2006,** *47*, 3426–3435.
18. Schmidt, D. F.; Clément, F.; Giannelis, E. On the Origins of Silicate Dispersion in Polysiloxane/Layered-Silicate Nanocomposites. *Adv. Funct. Mater.* **2006,** *16*, 417–425.
19. Andrews, R.; Jacques, D.; Rao, A. M.; Derbyshire, F.; Qian, D.; Fan, X.; Dickey, E. C.; Chen, J. Continuous Production of Aligned Carbon Nanotubes: A Step Closer to Commercial Realization. *Chem. Phys. Lett.* **1999,** *303*, 467–474.
20. Barber, A. H.; Cohen, S. R.; Wagner, H. D. Static and Dynamic Wetting Measurements of Single Carbon Nanotubes. *Phys. Rev. Lett.* **2004,** *92*, 186103.
21. Ci, L.; Suhr, J.; Pushparaj, V.; Zhang, X.; Ajayan, P. M. Continuous Carbon Nanotube Reinforced Composites. *Nano Lett.* **2008,** *8*, 2762–2766.
22. Garcia, E. J.; Hart, A. J.; Wardle, B. L.; Slocum, A. H. Fabrication of Composite Microstructures by Capillarity-Driven Wetting of Aligned Carbon Nanotubes with Polymers. *Nanotechnology* **2007,** *18*, 165602.
23. Raravikar, N. R.; Schadler, L. S.; Vijayaraghavan, A.; Zhao, Y.; Wei, B.; Ajayan, P. M. Synthesis and Characterization of Thickness-Aligned Carbon Nanotube-Polymer Composite Films. *Chem. Mater.* **2005,** *17*, 974–983.
24. Chen, W.; Qu, L.; Chang, D.; Dai, L.; Ganguli, S.; Roy, A. Vertically-Aligned Carbon Nanotubes Infiltrated with Temperature-Responsive Polymers: Smart Nanocomposite Films for Self-Cleaning and Controlled Release. *Chem. Commun.* **2008,** 163.
25. Cao, A.; Dickrell, P. L.; Sawyer, W. G.; Ghasemi-Nejhad, M. N.; Ajayan, P. M. Super-Compressible Foamlike Carbon Nanotube Films. *Science* **2005,** *310*, 1307–1310.
26. Suhr, J.; Koratkar, N.; Keblinski, P.; Ajayan, P. Viscoelasticity in Carbon Nanotube Composites. *Nat. Mater.* **2005,** *4*, 134–137.
27. Putz, K. W.; Palmeri, M. J.; Cohn, R. B.; Andrews, R.; Brinson, L. C. Effect of Cross-Link Density on Interphase Creation in Polymer Nanocomposites. *Macromolecules* **2008,** *41*, 6752–6756.
28. Xu, J.; Razeeb, K. M.; Roy, S. Thermal Properties of Single Walled Carbon Nanotube-Silicone Nanocomposites. *J. Polym. Sci., Polym. Phys.* **2008,** *46*, 1845–1852.
29. Mark, J. E. *Polymer Data Handbook*, 2nd ed.; Oxford University Press: New York, 2009.
30. Bansal, A.; Yang, H.; Li, C.; Cho, K.; Benicewicz, B. C.; Kumar, S. K.; Schadler, L. S. Quantitative Equivalence between Polymer Nanocomposites and Thin Polymer Films. *Nat. Mater.* **2005,** *4*, 693–698.
31. Sun, G.; Chen, G.; Liu, Z.; Chen, M. Preparation, Crystallization, Electrical Conductivity and Thermal Stability of Syndiotactic Polystyrene/Carbon Nanotube Composites. *Carbon* **2010,** *48*, 1434–1440.
32. Zhang, D.; Meyer, H. Molecular Dynamics Study of Polymer Crystallization in the Presence of a Particle. *J. Polym. Sci., Polym. Phys.* **2007,** *45*, 2161–2166.
33. Dollase, T.; Wilhelm, M.; Spiess, H.; Yagen, Y.; Yerushalmi-Rozen, R.; Gottlieb, M. Effect of Interfaces on the Crystallization Behavior of PDMS. *Interface Sci.* **2003,** *11*, 199–209.
34. Wei, C.; Srivastava, D.; Cho, K. Structural Ordering in Nanotube Polymer Composites. *Nano Lett.* **2004,** *4*, 1949–1952.